Interface-Induced Morphology Transition in Triblock Copolymer Films Swollen with Low-Molecular-Weight Homopolymer[†]

P. Müller-Buschbaum,*,‡ L. Schulz,‡,§ E. Metwalli,‡ J.-F. Moulin,‡,‖ and R. Cubitt⊥

Technische Universität München, Physikdepartment E13, James-Franck-Strasse 1, 85747 Garching, Germany, Université de Fribourg, Physics Department, Chemin du Musée 3, 1700 Fribourg, Switzerland, Institut für Werkstoffforschung, GKSS-Forschungszentrum Geesthacht GmbH, 21502 Geesthacht, Germany, and Institut Laue-Langevin, 6 rue Jules Horowitz, bp 156, 38042 Grenoble, France

The morphology transition due to midblock swelling with low-molecular-weight homopolymer polystyrene of an ABA-type triblock copolymer polyparamethylstyrene-*block*-polystyrene-block-polyparamethylstyrene at the buried silicon substrate interface is studied as a function of different substrate surface treatments. With grazing incidence small-angle neutron scattering (GISANS), high interface sensitivity is reached. The powderlike oriented lamellar structure in the bulk becomes oriented along the surface normal in the vicinity of the substrate. A transition of the lamellar into a cylinder phase at the polymer−silicon interface is probed with GISANS. The transition is induced by the addition of the homopolymer, but the modification of the short-ranged interface potential of the substrate influences the amount of homopolymer that is necessary for this transition. Without and with 0.1 vol % added homopolymer, the lateral spacing is stretched at the interface as compared to the bulk whereas for a higher added amount of homopolymer no stretching occurs.

1. Introduction

In fundamental research as well as in applications, block copolymers continuously attract strong interest because of microphase-separation-driven ordering on the nanoscale. Examples of these nanostructured morphologies are spheres or cylinders of the minority monomer species in a matrix of the majority monomer species for asymmetric copolymers and the lamellar structure for symmetric ones. The competition between enthalpic (incompatibility due to repulsive interaction) and entropic (chain packing effects) contributions determines the corresponding phase diagram, which to great extent was investigated for copolymers built from immiscible monomer units (A and B) in AB-type systems.[1−6] Increasing complexity by adding a third monomer unit C to an ABC-type triblock copolymer significantly enriches the number of possible structures, and rather complicated phase diagrams result.[7−11] In the case of a triblock copolymer of the ABA type, the situation simplifies. In contrast to AB-type diblock copolymers, the mean-field phase diagrams

of ABA-type triblock copolymers are highly asymmetric as a result of the higher entropic penalty in deforming the central B blocks so as to accommodate the two outer blocks into the A domains.[12]

With respect to applications, AB-type block copolymer systems are suffering from a lack of mechanical integrity. In an ordered diblock copolymer, each block behaves as a polymer tail, which is grafted at one end to the interface that divides neighboring microdomains. The mechanical integrity of a molten diblock copolymer is therefore the result of only block entanglement within each of the A and B microdomains. In contrast, ABA-type triblock copolymers exhibit a certain fraction of B chains bridging between neighboring domains.[12−14] The midblock of a triblock copolymer, covalently linked to both end blocks, is thereby establishing a physically cross-linked network that possesses greater strength than a diblock copolymer of comparable composition and half molecular weight. In the melt state, this system is much more difficult to pull apart even as a liquid because of the presence of these bridges.[15] The conformation of the midblock thus contributes to the mechanical behavior, and the fraction of bridged over looped chains becomes important.

Of particular interest is the use of an additive to alter the morphology and mechanical properties of linear block copolymers to overcome the normally required tailored synthesis of application-specific copolymer molecules. The characteristics of a microphase-ordered block copolymer can be systematically modified through physical blending with a (non)preferential solvent,[16−21] a parent homopolymer,[22−30] or a second copoly-

[†] Part of the Neutron Reflectivity special issue.

* Corresponding author: Phone: +49 89 289 12451. Fax: +49 89 28912473. E-mail: muellerb@ph.tum.de.

‡ Technische Universität München.

§ Université de Fribourg.

‖ Institut für Werkstoffforschung.

⊥ Institut Laue-Langevin.

(1) Hamley, I. W. *The Physics of Block Copolymers*; Oxford University Press: Oxford, U.K., 1998.

(2) Fredrickson, G. H. *Macromolecules* **1987**, *20*, 2535.

(3) Floudas, G.; Hadjichrisitidis, N.; Iatrou, H.; Pakula, T.; Fischer, E. W. *Macromolecules* **1994**, *27*, 7735.

(4) Förster, S.; Khandpur, A. K.; Zhao, J.; Bates, F. S.; Hamley, I. W.; Ryan, A. J.; Bras, W. *Macromolecules* **1994**, *27*, 6922.

(5) Khandpur, A. K.; Förster, S.; Bates, F. S.; Hamley, I. W.; Ryan, A. J.; Bras, W.; Almdal, K.; Mortensen, K. *Macromolecules* **1995**, *28*, 8796.

(6) Alexandridis, P.; Olsson, P.; Lindman, B. *Langmuir* **1998**, *14*, 2627.

(7) Alexandridis, P.; Spontak, R. J. *Curr. Opin. Colloid Interface Sci.* **1999**, *4*, 130.

(8) Schmalz, H.; van Guldener, V.; Gabrielse, W.; Lange, R.; Abetz, V. *Macromolecules* **2002**, *35*, 5491.

(9) Abetz, V.; Markgraf, K.; Rebizant, V. *Macromol. Symp.* **2002**, *177*, 139.

(10) Bohbot-Raviv, Y.; Wang, Z. G. *Phys. Rev. Lett.* **2000**, *85*, 3428.

(11) Bang, J.; Kim, S. H.; Drockenmuller, E.; Misner, M. J.; Russell, T. P.; Hawker, C. J. *J. Am. Chem. Soc.* **2006**, *23*, 7622.

(12) Mayes, A. M.; de la Cruz, M. O. *J. Chem. Phys.* **1991**, *95*, 4670.

(13) Matsen, M. W.; Schick, M. *Macromolecules* **1994**, *27*, 187–192.

(14) Watanabe, H. *Macromolecules* **1995**, *28*, 5006.

(15) Chen, C.-M.; MacKintosh, F. C.; Williamst, D. R. M. *Langmuir* **1995**, *11*, 2471.

(16) Hanley, K. J.; Lodge, T. P. *J. Polym. Sci., Part B: Polym. Phys.* **1998**, *36*, 3101.

(17) Hanley, K. J.; Lodge, T. P.; Huang, C. I. *Macromolecules* **2000**, *33*, 5918.

(18) Laurer, J. H.; Khan, S. A.; Spontak, R. J.; Satkowski, M. M.; Grothaus, J. T.; Smith, S. D.; Lin, J. S. *Langmuir* **1999**, *15*, 7947.

(19) Knoll, A.; Horvat, A.; Lyakhova, K. S.; Krausch, G.; Sevink, G. J. A.; Zvelindovsky, A. V.; Magerle, R. *Phys. Rev. Lett.* **2002**, *89*, 035501.

mer.[31−34] The addition of homopolymer molecules to a microphase-ordered block copolymer either swells the host microdomains or induces a morphological transformation to a nanostructure with different interfacial curvature. In contrast to AB-type diblock copolymer/homopolymer blends, the addition of a midblock-associating homopolymer to an ordered ABA-type triblock copolymer is expected to have a far more significant effect on the properties and phase behavior of the resulting copolymer/homopolymer blend as a result of the decrease in the fraction of bridged midblocks.[35]

The molecular weight of added homopolymer in relation to that of the compatible copolymer block and the composition of the blend expressed in terms of the homopolymer mass percent turned out to be important parameters.[36] Miscibility is usually retained in such blends if the ratios of the molecular weight of the added homopolymer to the molecular weight of the compatible block and the added amount of homopolymer are relatively small. An increase in either or both of these quantities ultimately induces macrophase separation at equilibrium.

As compared to bulk morphologies, in thin films the interaction with the confining asymmetric wall (substrate and air interface) typically complicates the behavior and can result in modification of the morphologies. Usually preferential wetting of one of the blocks at an interface leads to the parallel orientation of the microdomains, and when the thickness of the film is incommensurate with the lamellar (or cylindrical/spherical) period, quantization of the film thickness takes place by the formation of terraces. In triblock copolymer films in addition to the comparable behavior of surface-induced ordering,[37−41] deviations from the bulk structure were reported.[42−45] The wall interaction

can introduce a change in the characteristic spacing, such as shrinkage or stretching of the domain spacing, or it can cause morphology transitions.

One area of application is focusing on thin films of highly ordered block copolymers, which can be used to fabricate high-density arrays for microfiltration, data storage, microelectronics, and photonics applications.[46,47] For such thin films, the determination of the surface morphology with imaging techniques such as atomic force microscopy (AFM) and depth profiling with X-ray or neutron reflectivity is sufficient to determine the necessary structure information. However, for other applications related to thick copolymer films, which are used because of their special mechanical properties (e.g., in pressure-sensitive adhesives[48]), the structure determination is more complicated. Such thick films are typically characterized by a powderlike random orientation of the microphase-ordered block copolymer and, as detected recently, a well-ordered interface structure that is perpendicular to the interface plane.[45] Experimental difficulties in selectively addressing such buried interfaces, meaning the structure of the copolymer at the substrate, were overcome by the use of grazing incidence small-angle neutron scattering (GISANS).[49−52]

Within this investigation, we apply GISANS to probe the effect of blending an ABA-type triblock copolymer with a B-type homopolymer in bulky films, thereby addressing the area of thick films. In comparison to the volume structure inside the films, the interface structure is characterized as a function of three different short-ranged interactions installed with different surface treatments.[53] The nanostructure due to microphase separation of the triblock copolymer is measured. Morphological transitions in the interface structure are observed, which have no counterpart in the film volume.

This article is structured as follows. The introduction is followed by an experimental section describing the sample preparation and the techniques used. The section results and discussion are followed by a summary.

2. Experimental Section

Sample Preparation. A modification of the short-range interface potential of the silicon substrate was introduced by applying three different surface treatments.[53] The Si substrates were treated either in an acid bath or a base bath or a polystyrene (PS) layer was grafted onto the Si surface. After 15 min at 80 °C in the acid bath (consisting of 100 mL of 80% H_2SO_4, 35 mL of H_2O_2, and 15 mL of deionized water) the substrates were taken out, rinsed in deionized water, and blown dried with compressed nitrogen. In the base bath, the samples were sonicated in dichloromethane for 5 min, rinsed with Millipore water, and kept for 2 h in an oxidation bath at 75 °C consisting of 1400 mL of Millipore water, 120 mL of H_2O_2, and 120 mL of NH_3. Thereafter, the samples were stored in Millipore water. Directly before spin-coating, the substrates were rinsed with Millipore water at least 5 times to remove possible traces of the oxidation bath and were blown dry with nitrogen as well. The acid and base treatments resulted in a thin silicon oxide layer (thickness of 1 nm) covering the Si surface. The polystyrene (PS) layer was grafted via a grafting-to procedure by annealing a spin-coated layer of the corresponding

(20) Gong, Y.; Hu, Z.; Chen, Y.; Huang, H.; He, T. *Langmuir* **2005**, *21*, 11870–11877.

(21) van Zoelen, W.; Asumaa, T.; Ruokolainen, J.; Ikkala, O.; ten Brinke, G. *Macromolecules* **2008**, *41*, 3199.

(22) Green, P. F.; Russell, T. P. *Macromolecules* **1991**, *24*, 2931.

(23) Xu, T.; Goldbach, J. T.; Misner, M. J.; Kim, S.; Gibaud, A.; Gang, O.; Ocko, B.; Guarini, K. W.; Black, C. T.; Hawker, C. J.; Russell, T. P. *Macromolecules* **2004**, *37*, 2972.

(24) Winey, K. I.; Thomas, E. L.; Fetters, L. J. *J. Chem. Phys.* **1991**, *95*, 9367.

(25) Kimishima, K.; Hashimoto, T.; Han, C. D. *Macromolecules* **1995**, *28*, 3842.

(26) King, M. R.; White, S. A.; Smith, S. D.; Spontak, R. J. *Langmuir* **1999**, *15*, 7886.

(27) Laurer, J. H.; Khan, S. A.; Spontak, R. J.; Satkowski, M. M.; Grothaus, J. T.; Smith, S. D.; Lin, J. S. *Langmuir* **1999**, *15*, 7947.

(28) Bodycomb, J.; Yamaguchi, D.; Hashimoto, T. *Macromolecules* **2000**, *33*, 5187.

(29) Roberge, R. L.; Patel, N. P.; White, S. A.; Thongruang, W.; Smith, S. D.; Spontak, R. J. *Macromolecules* **2002**, *35*, 2268.

(30) Jeong, U.; Ryu, D. Y.; Kho, D. H.; Lee, D. H.; Kim, J. K.; Russell, T. P. *Macromolecules* **2003**, *36*, 3626.

(31) Spontak, R. J.; Fung, J. C.; Braunfeld, M. B.; Sedat, J. W.; Agard, D. A.; Kane, L.; Smith, S. D.; Satkowski, M. M.; Ashraf, A.; Hajduk, D. A.; Gruner, S. M. *Macromolecules* **1996**, *29*, 4494.

(32) Papadakis, C. M.; Mortensen, K.; Posselt, D. *Eur. Phys. J. B* **1998**, *4*, 325.

(33) Goldacker, T.; Abetz, V. *Macromolecules* **1999**, *32*, 5165.

(34) Court, F.; Hashimoto, T. *Macromolecules* **2001**, *34*, 2536.

(35) Kane, L.; Norman, D. A.; White, S. A.; Matsen, M. W.; Satkowski, M. M.; Smith, S. D.; Spontak, R. J. *Macromol. Rapid Commun.* **2001**, *22*, 281.

(36) Quan, X.; Gancarz, I.; Koberstein, J. T.; Wignall, G. D. *Macromolecules* **1987**, *20*, 1431.

(37) Sakurai, S.; Aida, S.; Okamoto, S.; Ono, T.; Imaizumi, K.; Nomura, S. *Macromolecules* **2001**, *34*, 3672.

(38) Finne, A.; Andronova, N.; Albertsson, A. C. *Biomacromolecules* **2003**, *4*, 1451.

(39) Shin, D.; Shin, K.; Aamer, K. A.; Tew, G. N.; Russell, T. P.; Lee, J. H.; Jho, J. Y. *Macromolecules* **2005**, *38*, 104.

(40) Wu, W.; Huang, J.; Jia, S.; Kowalewski, T.; Matyjaszewski, K.; Pakula, T.; Gitsas, A.; Floudas, G. *Langmuir* **2005**, *21*, 9721.

(41) Müller-Buschbaum, P.; Maurer, E.; Bauer, E.; Cubitt, R. *Langmuir* **2006**, *22*, 9295.

(42) Rehse, N.; Knoll, A.; Konrad, M.; Magerle, R.; Krausch, G. *Phys. Rev. Lett.* **2001**, *87*, 035505.

(43) Krausch, G.; Magerle, R. *Adv. Mater.* **2002**, *14*, 1579.

(44) Epps, T. H., III; DeLongchamp, D. M.; Fasolka, M. J.; Fischer, D. A.; Jablonski, E. L. *Langmuir* **2007**, *23*, 3355.

(45) Müller-Buschbaum, P.; Schulz, L.; Metwalli, E.; Moulin, J. F.; Cubitt, R. *Langmuir* **2008**, *24*, 7639.

(46) Fasolka, M. J.; Mayes, A. M. *Annu. Rev. Mater. Res.* **2001**, *31*, 323–355.

(47) Segalman, R. A. *Mater. Sci. Eng. R* **2005**, *48*, 191–226.

(48) Possart, W. *Adhesion*; Wiley-VCH: Weinheim, Germany, 2005.

(49) Müller-Buschbaum, P.; Gutmann, J. S.; Stamm, M. *Phys. Chem. Chem. Phys.* **1999**, *1*, 3857.

(50) Müller-Buschbaum, P.; Gutmann, J. S.; Cubitt, R.; Stamm, M. *Colloid Polym. Sci.* **1999**, *277*, 1193.

(51) Müller-Buschbaum, P.; Cubitt, R.; Petry, W. *Langmuir* **2003**, *19*, 7778.

(52) Wolff, M.; Magerl, A.; Zabel, H. *Eur. Phys. J. E* **2005**, *16*, 141.

(53) Müller-Buschbaum, P. *Eur. Phys. J. E* **2003**, *12*, 443.

carboxy-terminated PS above the glass-transition temperature,[54] followed by a rinsing step to remove the excess material. By control of the annealing time, a PS-brush thickness of 5 nm was installed.

The static water contact angles measured after the different surface treatments are $\Theta = 0$ for the base cleaning, 20 for the acid cleaning, and 91° for the PS brush.

The selected triblock copolymer was polyparamethylstyrene-*block*-polystyrene-*block*-polyparamethylstyrene, denoted P(pMS-*b*-Sd8-*b*-pMS), with a fully deuterated polystyrene (PSd) middle block ($M_w = 140\,000$ g/mol), two equally sized protonated polyparamethylstyrene blocks (each with $M_w = 70\,000$ g/mol), and a total molecular weight of $M_w = 280\,000$ g/mol. It was prepared anionically (Polymer Standard Service, Mainz, Germany), resulting in a narrow molecular weight distribution of $M_w/M_n = 1.1$. The degree of polymerization of the PSd block compared to that of the total chain was $f_{PSd} = N_{PSd} = 0.51$. Thus, the internal nanostructure resulting from microphase separation in bulklike P(pMS-*b*-Sd8-*b*-pMS) films is a randomly oriented lamella with a powderlike orientation of the lamellar domains.

For blending, a homopolymer compatible with the midblock of the ABA-type triblock copolymer was chosen. Deuterated polystyrene (PSd) with a very low molecular weight of $M_w = 2300$ g/mol ($M_w/M_n = 1.05$) was used to avoid macrophase separation. Three different blending ratios with 0.1, 0.2, and 0.5 vol % added PSd were investigated. Triblock copolymer and homopolymer were blended in toluene solution and spin coated (1950 rpm for 30 s) onto the chemically modified SiO_x surface. Storage under a toluene vapor atmosphere (pressure $p = 0.8p_0$, temperature 296 K) was applied to allow the structure of the triblock copolymer/homopolymer blend films to come to equilibrium. After 20 h of storage, the samples were quenched in ambient air and examined.

Grazing Incidence Small-Angle Neutron Scattering Experiments. GISANS measurements were performed at the D22 beamline at the ILL neutron reactor (Grenoble). A wavelength of 0.6 nm (wavelength selector $\Delta\lambda/\lambda = 10\%$), extremely narrow cross-slits with typical openings of 1 mm, a sample−detector distance of 14.4 m, and a collimation of 17.6 m were used, resulting in an experimental resolution of 3×10^{-3} nm^{-1} in terms of the largest resolvable lateral structure. The background was minimized by the completely evacuated pathway except for a small region of ±10 mm in front of and behind the sample. Following the sample geometry, which is successfully used in neutron reflectometry,[55−57] the neutron beam impinges not from the polymer film surface but through the silicon (Si) substrate, as detailed in ref 45. The direct beam was blocked on the detector with a beamstop to reduce background. Details concerning the beamline are reported elsewhere.[58]

Two different angles of incidence were selected: (1) The volume structure of the blend film was probed at an angle of incidence ($\alpha_i = 0.718°$) above the critical angle of the SiO_x−polymer interface. (2) The interface structure was addressed at an extremely shallow angle of incidence ($\alpha_i = 0.067°$), which is significantly smaller than the critical angle of the SiO_x−polymer interface. The error in the angle of incidence was 0.008°. It was determined by the accuracy of the alignment that was given by the half size of a pixel of the detector at the given distance. The GISANS information in the recorded 2D intensity map (128 pixel × 128 pixel array, effective pixel size 8 × 8 mm^2) was extracted from slices parallel to the sample surface at the critical angle.[49−51] Statistics of these slices were improved by integrating the intensity over the two neighboring detector lines corresponding to $\Delta q_z = \pm 2.33 \times 10^{-2}$ nm^{-1}.

Typical counting times were on the order of hours to obtain reasonable statistics.

X-ray Reflectivity Measurements. With a laboratory X-ray source (Θ-Θ reflectometer Seifert XRD 3003TT), reflectivity measurements of the chemically modified substrates and the triblock copolymer/homopolymer blend films were performed. A Ge(110) channel-cut crystal is used to monochromatize the beam (wavelength of 0.154 nm). Samples were placed on a specially designed vacuum chuck and were measured in air. From the reflectivity curves of the annealed films, a total film thickness of 880 ± 10 nm was detected. The given error accounts for deviations between different samples of various compositions. The density was close to the mean density of both components PSd and PpMS, and because of the weak X-ray scattering contrast, resolution of the internal order was not possible and no Bragg peaks were observed.

Atomic Force Microscopy. With atomic force microscopy (AFM), the chemically modified substrates and the triblock copolymer/homopolymer blend films were investigated. A PARK Autoprobe CP atomic force microscope was operated with silicon−gold-coated conical cantilevers (resonance frequencies at approximately $f = 60$ kHz and a spring constant of approximately 2.1 N m^{-1}). Upon scale up to 10 μm, the surfaces were homogeneous and showed no marked features. Because of the missing mechanical contrast between both components PSd and PpMS, however, AFM gives no access to the nanoscale structure introduced by microphase separation. Moreover, it was not possible to access the buried SiO_x−polymer interface with AFM because attempts to delaminate the film from the substrate failed.

3. Results and Discussion

From previous work,[45] the volume and interface structure of the neat triblock copolymer on SiO_x substrates is known: (1) Base cleaning was demonstrated to create a nonselective, neutral wall for the two blocks PSd and PpMS of the triblock copolymer. It results in a hydrophilic substrate surface (water contact angle $\Theta = 0°$) that is unfavorable for both blocks, but because of the large film thickness, dewetting is suppressed and both blocks stay equally at the interface. No preferential wetting occurs, and the chain remains unstretched but oriented perpendicular to the interface.[45] (2) The PS brush acts like a midblock selective wall because of the preferential substrate interaction. This causes a stretching of the midblock of the triblock copolymer accompanied by an increase in disorder, whereas in the interface near region the order is improved by the alignment of the chains as compared to that in the bulk.[45] (3) The acid treatment presents less-hydrophilic surfaces, which favors wetting with blocks of lower surface tension and the end blocks for the given triblock copolymer. In contrast to diblock copolymer films, no parallel orientation with respect to the substrate resulted, and again a perpendicularly aligned lamella is found.[45] As a consequence, irrespective of the surface treatment in the neat triblock copolymer films, a lamellar structure oriented perpendicular to the interface was always present at the interface. Within the present work, we now investigate if this lamellar structure remains stable upon addition of homopolymer or if morphology transitions happen in the bulk of the film or at the interface.

GISANS Analysis. The GISANS analysis is performed with fits in the framework of the distorted wave Born approximation (DWBA). In a simplified approach, the differential cross-section can be approximated for the large film thickness, and the current geometry can be approximated by the diffuse scattering from one rough interface[59]

$$\frac{d\sigma}{d\Omega} = A(Nb)^2 |T_i|^2 |T_f|^2 F(\vec{q})$$

Because α_i and α_f are fixed in GISANS, the Fresnel transmission functions $T_{i,f}$ and the illuminated surface area A as

(54) Ionov, L.; Sidorenko, A.; Stamm, M.; Minko, S.; Zdyrko, B.; Klep, V.; Luzinov, I. *Macromolecules* **2004**, *37*, 7421.

(55) Rennie, A. R.; Lee, E. M.; Simister, E. A.; Thomas, R. K. *Langmuir* **1990**, *6*, 1031.

(56) Lu, J. R.; Thomas, R. K. *J. Chem. Soc., Faraday Trans.* **1998**, *94*, 995.

(57) Gutberlet, T.; Klosgen, B.; Krastey, R.; Steitz, R. *Adv. Eng. Mater.* **2004**, *6*, 832.

(58) Büttner, H. G.; Lelievre-Berna, E.; Pinet, F. *Guide to Neutron Research Facilities at the ILL* **1997**, 32.

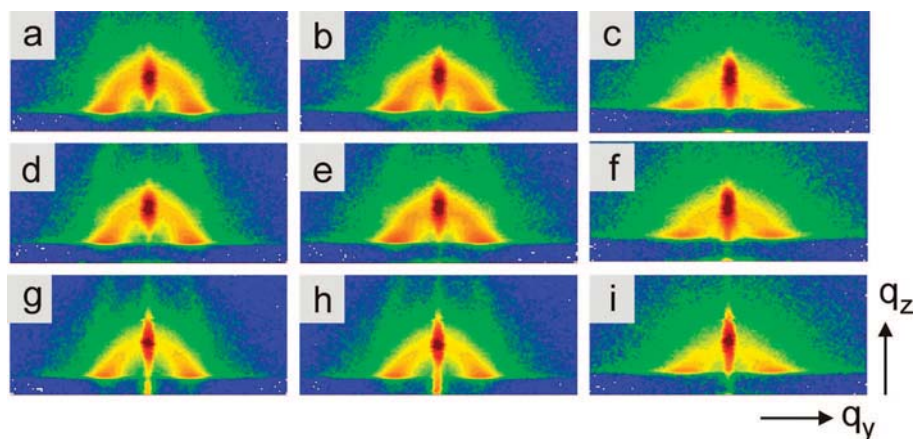(59) Leroy, F.; Lazzari, R.; Renaud, G. *Surf. Sci.* **2007**, *601*, 1915.

Figure 1. Two-dimensional scattering patterns recorded in the GISANS measurements (for an angle of incidence of $\alpha_i > \alpha_c$) for the three different surface treatments, from top to bottom: (a−c) acid cleaning, (d−f) base cleaning, and (g−i) PS- brush. In the left column (a, d, g) 0.1, in the middle column (b, e, h) 0.2, and in the right column (c, f, i) 0.5 vol % PSd was added to the triblock copolymer. The intensity is shown with logarithmic color coding.

well as the coherent scattering length density (SLD) step at the Si−polymer interface Nb act only as overall scaling factors, and the diffuse scattering factor $F(q)$ is directly detected. The diffuse scattering factor is assumed to be proportional to the form factor of individual objects $P(q)$ and to the structure factor $S(q)$ describing the lateral correlation between these objects, with N being the number of objects:

$$F(\vec{q}) \approx NP(\vec{q})\, S(\vec{q})$$

In this model, $F(q)$ takes into account the microphase-ordered block copolymer structure, such as lamella or hexagonally ordered cylinders. From the microphase separation structure with dominant (lamellar or cylinder) spacing, a structure factor contribution arises. Disorder is introduced with a Lorentzian-type probability distribution of the nearest-neighbor distances. With increasing width of the distribution, the Bragg peaks broaden, and higher-order Bragg peaks are damped out. To account for the polydispersity of the domains in the form factor as well, a Lorentzian distribution of sizes is assumed. Polydispersity causes a strong smearing of the form factor contribution. Moreover, the resolution function of the experimental setup is taken into account.

Volume Structure. The bulk film structure is addressed by selecting an angle of incidence ($\alpha_i = 0.718°$) well above the critical angle of the SiO_x−polymer interface (which is $\alpha_c = 0.24°$ as calculated from the coherent SLD step at the SiO_x−polymer interface Nb = 1.505×10^{-6} $Å^{-2}$ [60]).

To define a coordinate system, the x axis was directed along the incident beam, and the sample surface is defined as the (x, y)-plane. Thus, the (x, z)-plane denotes the plane of incidence and reflection. For the scattering vector $\mathbf{q} = (q_x, q_y, q_z)$, specular scattering is observed for $q_x = q_y = 0$ and $q_z > 0$. The specular peak fulfills the specular condition ($\alpha_i = \alpha_f$), and diffuse scattering intensity is observed for $q_x \neq 0$. Consequently, the 2D detector (Figure 1) contains diffuse scattering information. Neglecting a small q_x contribution, the 2D scattering pattern has a q_z dependence along lines perpendicular to the sample surface and a q_y dependence along lines parallel to the sample surface. Figure 1 shows the 2D GISANS pattern measured for the triblock copolymer/homopolymer blend films with different blend ratios and on differently treated silicon substrates. From left to right in each row, the amount of added PSd increases at a fixed chemical

surface modification. The top-row data were probed on acid-cleaned surfaces, the middle-row data were probed on base-cleaned surfaces, and the bottom-row data were probed on PS brushs. In general, the GISANS data show a more complicated intensity distribution than do standard SANS data.[41] The scattering data are symmetric with respect to the vertical center as a result of the rotational isotropy of the films. Characteristics features of the scattering intensity are well separated on the detector: a specular peak (in the center of the detector) and a Yoneda peak with its Bragg rods (streaks in the top part of the detector) and ring-shaped intensity maximum. From the presence of this ring-shaped intensity, the typically observed powderlike random orientation of the microphase-ordered block copolymer is confirmed.

For in-depth analysis, selected line cuts are compared in Figure 2. Within the resolved range of lateral structures for all, three Bragg-type contributions are identified. One weak intensity maximum occurs at small q_y values (marked with Λ in Figure 2a), corresponding to an in-plane length of 250 nm. It is attributed to a superstructure, perhaps indicating the domain size, that had been observed in neat triblock copolymer films as well.[41,45] Within the domains, the lamellae are well-oriented, whereas the orientation is random between different domains. Toward larger q_y values, two more peaks are found. One peak is very strong in intensity (marked with D_1 in Figure 2a), and one peak is extremely weak and shoulderlike in its shape (marked with D_2 in Figure 2a). Both resemble nanoscale microphase separation order. To extract the quantitative values of the in-plane structures and probe the corresponding morphology, the GISANS data are fitted. Irrespective of the added amount of homopolymer, a lamellar model of the microphase-ordered block copolymer structure was able to explain the data, and the peaks marked with D_1 and D_2 are identified as first- and second-order Bragg peaks (ratio 1:2).

When 0.1 vol % PSd are added (Figure 2a), all of the first-order Bragg peaks exhibit the same intensity within experimental error. The second-order Bragg peaks are very weak compared to those expected for nearly symmetric lamella (equal sizes in parts A and B perturbed by added homopolymer) and are due to the disorder in the system. From both the first- and second-order peaks, a corresponding bulk lamellar spacing of $L_O = 46.5 \pm 0.5$ nm of the swollen film is determined. Thus, the value is changed as compared to the bulk lamellar spacing $L_{bulk} = 48 \pm 3$ nm of the neat triblock copolymer.[45]
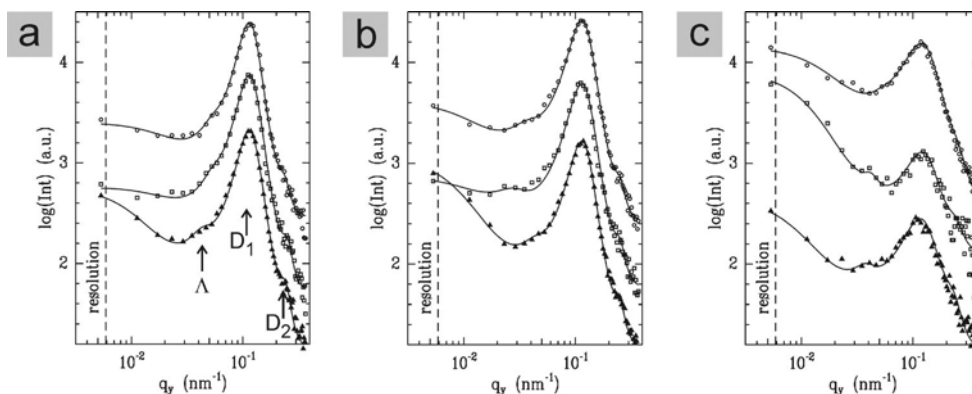
(60) Using the NIST tool at http://www.ncnr.nist.gov/resources/sldcalc.html .

Figure 2. Slices parallel to the sample surface at the critical angle α_c of the polymer against Si (shifted for clarity along the y axis): (a) 0.1, (b) 0.2, and (c) 0.5 vol % PSd added to the triblock copolymer. From top to bottom, acid-cleaning, base-cleaning, and PS brush data (symbols) are shown with a model fit (line). Bragg positions (Λ, D_1, and D_2) are indicated with small arrows, and the dashed line marks the resolution with respect to large lateral structures.

Figure 3. Lamellar spacing L_o of the bulk film probed as a function of the added amount of PSd, ϕ_{PS}, for the samples after acid cleaning (triangles) and base cleaning (squares) and for the PS brush surface (spheres). The dashed line shows the spacing with added homopolymer picturing the contraction upon addition of PSd.

By doubling the amount of added PSd (0.2 vol %, Figure 2b), no significant changes are obvious in the intensities, but Bragg peak positions D_1 and D_2 shift toward larger q_y values (i.e., smaller lateral structures). This shifting continues for 0.5 vol % PSd added; moreover, the Bragg peak intensities drop and the full width at half-maximum (fwhm) of the peaks increases significantly. Disorder has thus increased; correspondingly, the second-order Bragg peaks become even less pronounced (Figure 2c).

Figure 3 comprises the evolution of the lamellar spacing L_o of the bulk film probed as a function of the added amount of PSd, ϕ_{PS}, for the samples after acid cleaning (triangles) and base cleaning (squares) and for the PS brush surface (spheres). Data of the neat triblock copolymer were taken from ref 45 for comparison. With increasing amount of homopolymer added, the lamellar spacing becomes contracted. As is to be expected for a bulky film, these changes are independent of the chemical modifications at the SiO_x−polymer interface.

In the present investigation, we focus on the microphase-ordered block copolymer structure and thus the selected contrast PSd in P(pMS-*b*-Sd8-*b*-pMS), which prevent the determination of the distribution of the homopolymer inside the triblock copolymer. Thus we have no access to information about the distribution of PSd in the midblock of the triblock. However, it was shown by Lee and co-workers[61] with neutron scattering experiments that the distribution of a low-molecular-weight midblock-associating homopolymer dissolved within a triblock
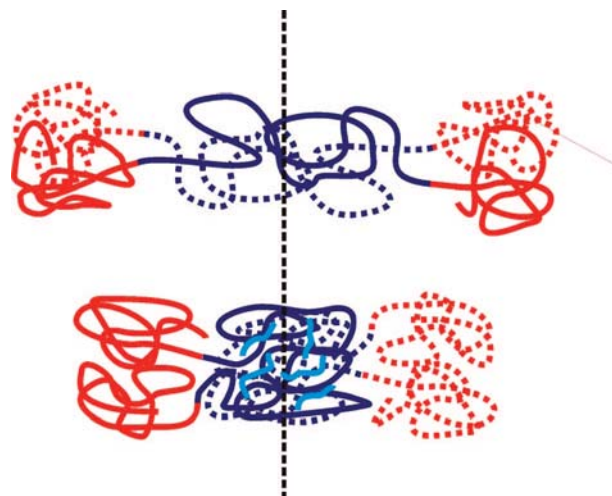

Figure 4. Possible scenarios arising with an ABA-type triblock copolymer chain: (top) net polymer in a bridged conformation and (bottom) looped conformation swollen with a low-molecular-weight homopolymer. In each sketch, two chains are shown (one by a solid line and one by a dashed line). The vertical dashed line indicates the middle of the chain to illustrate the contraction upon swelling.

copolymer is inhomogeneous. There is a strong tendency for the homopolymer to localize preferentially at the center of the midblock microdomain and the microdomain structure contracts. The preferential positioning is driven by the release of constraints on the normally extended midblock sequences in the bridged conformation. Constraints due to looping are realized in the looped conformation. Thus the localization of homopolymer at the center of the lamellar microdomains can ease these conformational constraints, thereby accounting for the contraction in the average lamellar thickness observed in our GISANS investigation. According to self-consistent field theory (SCFT)[62] and supported by experiments,[14] the bridging fraction lies between 0.40 and 0.45 for copolymers of modest incompatibility. The remaining fraction is in the looped conformation. Figure 4 shows both conformations. Moreover, it illustrates the contraction of the lamella upon the incorporation of low-molecular-weight ho-mopolymer. As an example, the bridged conformation is shown in the neat state, and the looped conformation is shown in the swollen state. Of course, the inverted scenario is present in the sample as well: in the neat state, the copolymer has a looped

(61) Lee, S. H.; Koberstein, J. T.; Quan, X.; Gancarz, I.; Wignall, G. D.; Wilson, F. C. *Macromolecules* **1994**, *27*, 3199.

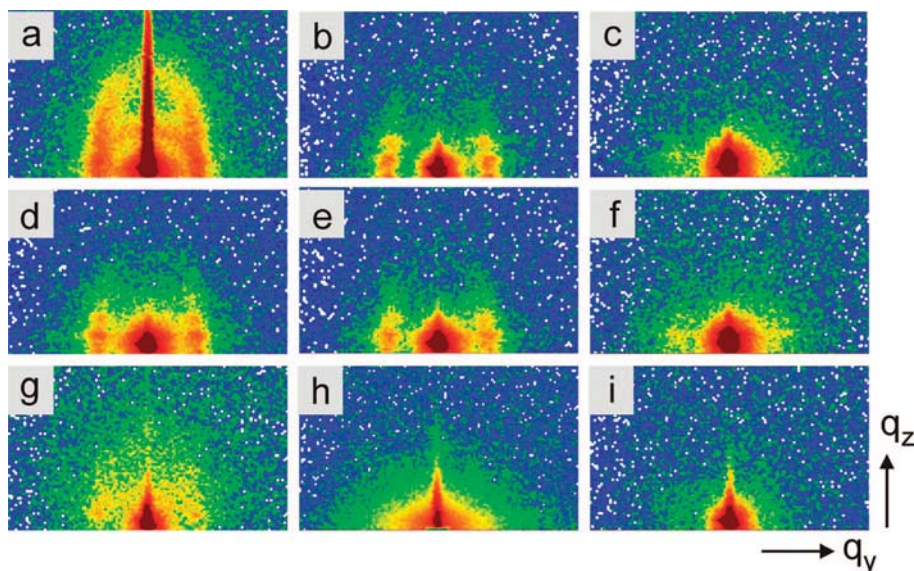(62) Matsen, M. W. *J. Chem. Phys.* **1995**, *102*, 3884.

Figure 5. Two-dimensional scattering patterns recorded in the GISANS measurements (for an angle of incidence of $\alpha_i < \alpha_c$) for the three different surface treatments, from top to bottom: (a−c) acid-cleaned, (d−f) base-cleaned, and (g−i) PS brush. In the left column (a, d, g) 0.1, in the middle column (b, e, h) 0.2, and in the right column (c, f, i) 0.5 vol % PSd were added to the triblock copolymer. The intensity is shown with logarithmic color coding.

conformation, and the swollen state of the bridged conformation results in a contraction.

However, in the system P(pMS-*b*-Sd8-*b*-pMS)/PSd no morphological transition occurs in the bulky films, whereas in other systems such a transition was observed. For example, poly(styrene-*block*-isoprene-*block*-styrene) triblock copolymers with block masses of 30 000 (PS) and 51 00 (PI) g/mol blended with a high-molecular-weight homopolyisoprene (30 000 g/mol) retained a lamellar morphology for up to 54 wt % added PI but underwent a morphological transition at higher amounts.[63] Thus, it is very likely that the smaller chemical difference between blocks PSd and PpMS as compared to other systems such as PS and PI or PS and PMMA might be attributed to keeping the lamellar morphology unchanged although the midblock is significantly swollen by homopolymer. It should be noted that for even larger amounts of PSd added to triblock copolymer P(pMS-*b*-Sd8-*b*-pMS) macrophase separation occurs and isolated domains of homopolymer and copolymer without homopolymer result.

Interface Structure. With decreasing angle of incidence, the scattering depth of the GISANS signal is reduced as well. Thus, to address the SiO_x−polymer interface only, it is advantageous to operate a very shallow angle of incidence. An angle of incidence of $\alpha_i = 0.067°$, well below the critical angle of the SiO_x−polymer interface, has been selected. It corresponds to a scattering depth of only 24 nm, which means that the obtained signal contains an average structure weighted by an exponential of this characteristic depth. Because of the system under investigation, for smaller angle of incidence, which are very difficult to handle in the GISANS experiment, no further significant reduction of the scattering depth beyond 24 nm would have been possible. Thus, the selected angle of incidence is a good compromise between a feasible scattering experiment and the smallest possible scattering depth.

The corresponding 2D GISANS pattern measured for the triblock copolymer/homopolymer blend films with different blend ratios and on differently treated silicon substrates are shown in

Figure 5. Again, from left to right in each row the amount of added PSd increases at a fixed chemical surface modification. The top-row data were probed on acid-cleaned surfaces, the middle-row data were probed on based-cleaned surfaces, and the bottom-row data were probed on PS brushs. Because of the small angle of incidence, the specular peak is located at the very bottom of the detector.

In contrast to the bulk-sensitive GISANS data recorded at a large angle of incidence (Figure 1), which all appear to be quite similar in their 2D patterns, strong changes in the 2D intensity distributions are obvious in Figure 5. For films with 0.1 vol % PSd added, well-pronounced features in the 2D intensity distribution can be seen in Figure 5, indicating that the structure at the SiO_x−polymer interface exhibits the highest order in these films. Upon adding more PSd, the side maxima decay in intensity because of an increase in the disorder of the structure at the interface. The same trend holds for replacing the acid-cleaned with the basic-cleaned with the PS brush.

Selected line cuts from the 2D intensities are compared in Figure 6. As for the bulk-sensitive GISANS measurements, in the interface-sensitive data three Bragg-type contributions are identified and marked with Λ, D_1, and D_2 in Figure 6a. Thus, at the interface a superstructure, indicating a domain size, and a nanoscale structure from the microphase-ordered block copolymer structure exist. The lateral extension of the superstructure is identical to that in the bulk with an in-plane length of 250 nm, and the nanoscale structure yields first- and second-order Bragg peaks (marked with D_1 and D_2 in Figure 6a). As a consequence, the triblock copolymer/homopolymer blend films exhibit a microphase-ordered structure that is oriented perpendicular to the interface. In this respect, the addition of PSd to the neat triblock copolymer did not change the structure.[42] However, this type of morphology is influenced by adding homopolymer whereas for the neat triblock copolymer lamellar morphology describes the microphase-ordered block copolymer structure.[45] Upon addition of homopolymer, this is no longer valid for all blending ratios. For some surface treatments and blending ratios, a better fitting of the Bragg peak positions is obtained with a hexagonally ordered cylinder structure. Table 1

(63) Norman, D. A.; Kane, L.; White, S. A.; Smith, S. D.; Spontak, R. J. *J. Mater. Sci. Lett.* **1998**, *17*, 545.
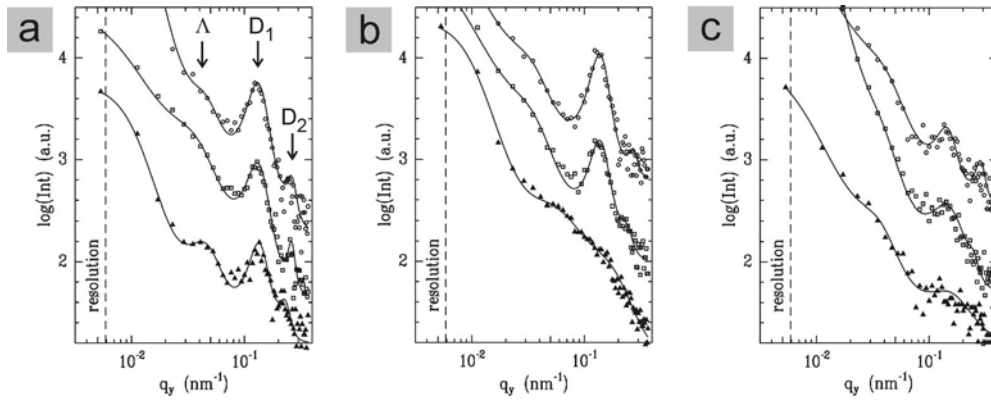
Figure 6. Slices parallel to the sample surface at the critical angle α_c of the polymer against Si (shifted for clarity along the y axis): (a) 0.1, (b) 0.2, and (c) 0.5 vol % PSd added to the triblock copolymer. From top to bottom, the data (dots) of acid cleaning, base cleaning, and the PS brush are shown with a model fit (line). Bragg positions (Λ, D_1, and D_2) are indicated with small arrows, and the dashed line marks the resolution with respect to large lateral structures.

Table 1. Detected Interface Morphology of the Triblock Copolymer Film as a Function of the Amount of Added PSd and Surface Treatment[a]

	0.0 vol % PSd	0.1 vol % PSd	0.2 vol % PSd	0.5 vol % PSd
acid	L	L	L	L
base	L	L	H	H
PS brush	L	H	H	H

[a] L denotes a lamellar and H denotes a hexagonally ordered cylinder structure, both of which are oriented perpendicular to the interface.

gives an overview of the used morphologies. Only for acid cleaning is the lamellar morphology able to describe all blending ratios examined. For base cleaning for 0.2 and 0.5 vol % and for the PS brush for all three blend ratios, the cylinder morphology is better suited. However, again the presence of a microphase-ordered structure, which is oriented parallel to the interface, can be excluded because in this case no Bragg peaks in the q_y direction would have occurred but Bragg peaks in the q_z direction would have occurred.

In more detail, for 0.1 vol % PSd added, the structure at the interface is well ordered irrespective of the chemical surface treatment and as seen for the neat triblock copolymer because of the restriction of possible orientations by the presence of the interface, the degree of order is increased as compared to that of the bulk. As a consequence, the fwhm of the Bragg peak is decreased as compared to that in the bulk. Moreover, the second-order Bragg peaks are better pronounced, although the overall intensity is significantly smaller in the interface sensitive data as compared to the volume data because of the restricted scattering volume. When the PSd content is increased to 0.2 vol %, the interface structures become less ordered, an effect that at the PS−brush surface even results in the absence of well-developed Bragg peaks, whereas for acid cleaning and base cleaning mostly the second-order Bragg peaks are affected. For 0.5 vol % PSd added, the disorder further increases, as seen in the increase in the fwhm values of the Bragg peaks and the decrease in the Bragg peak intensities. In comparing the degree of order with the type of morphology, it appears that the lamellar structure exhibits larger order than does the cylinder morphology (cf. Table 1 and Figure 6).

In Figure 7, the determined lateral spacing values L_S of the triblock copolymer at the interface as a function of the added amount of PSd, ϕ_{PS}, for the samples after acid cleaning (triangles) and base cleaning (squares) and the PS brush surface (spheres) are shown. Again, for comparison the data of the neat triblock copolymer films are included from ref 45. In contrast to the chain
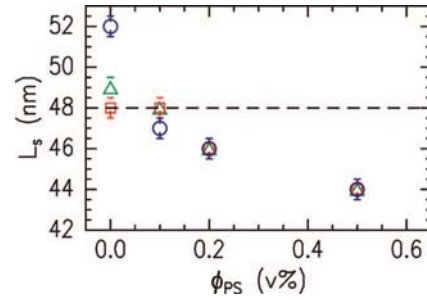

Figure 7. Lateral spacing L_S of the triblock copolymer at the interface as a function of the added amount of PSd ϕ_{PS} for the samples after acid cleaning (triangles) and base cleaning (squares) and the PS−brush surface (spheres). The dashed line shows the spacing with added homopolymer picturing the contraction upon addition of PSd.
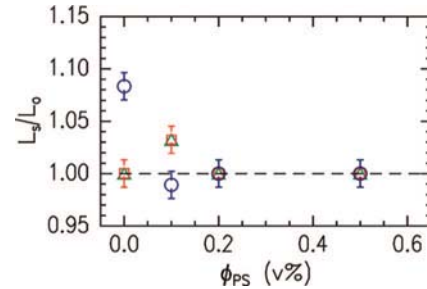

Figure 8. Lateral spacing L_S at the interface normalized by the bulk lamellar spacing L_O probed as a function of the added amount of PSd ϕ_{PS} for the samples after acid cleaning (triangles) and base-cleaning (squares) and the PS-brush surface (spheres). The dashed line shows the spacing with added homopolymer picturing the contraction upon addition of PSd.

stretching at the interface for the neat triblock copolymer, in the blend films at the interface shrinkage of lateral spacing occurs. Care must be taken because in addition a transition in the morphology is present (Table 1). For example, on the PS brush, which is the midblock-selective interface, the microphase-ordered structure for 0.1 vol % PSd added is cylinder-type and exhibits a smaller characteristic spacing as compared to the lamellar structure of the neat triblock copolymer.

To correlate the changes in the microphase-ordered block copolymer structure in the blend films at the interface with changes in the bulk structure of these films, Figure 8 shows the lateral spacing L_S at the interface normalized by the bulk lamellar spacing L_O probed as a function of the added amount of PSd, ϕ_{PS}. From

this normalization, it is obvious that strong changes happened in the neat triblock copolymer films and interface structures were found to be stretched up to 8%.[45] On the contrary, in the blend films this stretching decrease is nonexistent for 0.2 and 0.5 vol % homopolymer added, which could give the impression that no changes happen at the interface. However, the GISANS data show that a morphological transition is present at the interface and not in the film volume and hence the simple description with one characteristic lateral length as shown in Figure 8 can be very misleading. Therefore, the addition of homopolymer has two major effects. On one hand, it releases constraints on the normally extended midblock sequences in the bridged conformation, which result in an overall contraction of the chains and a reduced periodicity in the volume and at the interface (cf. Figure 3 and 7). On the other hand, it balances the interaction with the interface, thereby introducing morphological transitions from a lamellar into a cylindrical structure. Along this line, the type of wall installed by the different chemical treatments of the surfaces (neutral, midblock, and end-blocks favoring the wall) affects the amount of homopolymer that has to be added to introduce the morphological transition. On the midblock-selective wall (PS-selective wall), realized with the PS-brush surface, the midblock tries to maximize its contact with the wall, which in the neat triblock copolymer gives rise to strong chain stretching and, upon addition of some PS, allows the transition into a cylinder morphology of PpMS cylinders embedded in a PS matrix. On the neutral wall, realized with base cleaning, both blocks would like to avoid contact, which shifts the morphological transition to a higher concentration of PS. For the wall favoring end-block interaction (PpMS-selective wall), the addition of homopolymer unequal to the end blocks does not resulting in such a transition from lamella- to cylinder microphase-ordered block copolymer structure because the end block maximizes the contact. Therefore, the cylinder structure with PpMS cylinders in a PS matrix is unfavorable, and for the inverted structure of PS cylinders in a PpMS matrix, the ratio of PpMS components to PS does not match because of the addition of PS.

To our knowledge, so far no information on microphase-ordered block copolymer structures of triblock copolymer/homopolymer blends at the SiO_x−polymer interface is available in the literature. Only morphological changes as compared to the bulk structure near the free surface and due to confinement in very thin films have been reported. For example, in the case of poly(styrene-*block*-butadiene-*block*-styrene) triblock copolymer films on silicon, the cylindrical microdomain structure in the bulk was found to deviate from the near-surface morphology.[41] In the system of lamellar-forming triblock copolymer poly(styrene-*block*-butadiene-*block*-methylmethacrylate), the near-surface morphology was found to deviate as well.[43] In contrast, the strong polymer−polymer interactions of a poly(*n*-octadecyl methacrylate)-*b*-poly(tert-butyl acrylate)-*b*-poly(*n*-octadecyl methacrylate) triblock copolymer were accounted for in the good agreement between bulk and surface structures.[44] However, the P(pMS-*b*-Sd8-*b*-pMS) system is known not to exhibit morphological transitions in confined thin films or at the free surface.[41]

4. Conclusions

In summary, the powerful scattering technique GISANS has been used to probe microphase-separation-induced nanostructures in triblock copolymer/homopolymer blend films at buried interfaces. The regime of blend films that do not undergo macrophase separation is addressed by the use of a low-molecular-weight homopolymer and by restriction to an addition of up to 0.5 vol % homopolymer. Three different chemical treatments of the silicon substrates have been applied to achieve a neutral-, midblock-, and end-block-selective wall and detect the corresponding changes in the short-range part of the interface potential with respect to the structure and morphology of the blend films. Bulk conformational properties of polymer chains are modified by the addition of the homopolymer and by contact with the interface due to competition between the loss of entropy and the gain of internal energy. Therefore, changes in the bulk and interface structures occur. In the bulk blend films, the copolymer chains are contracted by enrichment of the homopolymer in the midblock domains and the resulting release of constraints. However, the lamellar morphology remains unchanged irrespective of the amount of added of homopolymer. In contrast, at the SiO_x−polymer interface morphological transitions are probed. The type of interface determines via its interaction with the blend, at which added amount of PSd ϕ_{PS} samples undergo the transition from lamella to cylinder structures. Without adding homopolymer, such a transition did not show up, which demonstrates that the changes in the wall interaction can be compensated for without morphological transitions for the particular triblock copolymer P(pMS-*b*-Sd8-*b*-pMS). This highlights the important role of entropy in such triblock copolymer films.